Conformations of Cyclic Octapeptides. 3. *cyclo*-(D-Ala-Gly-Pro-Phe)$_2$. Conformations in Crystals and a $T_{1\rho}$ Examination of Internal Mobility in Solution

Kenneth D. Kopple,*† Krishna K. Bhandary,‡ Gopinath Kartha,‡,§ Yu-Sen Wang,‖ and Kumarapuram N. Parameswaran‖

Contribution from the Department of Chemistry, Illinois Institute of Technology, Chicago, Illinois 60616, and Biophysics Department, Roswell Park Memorial Institute, Buffalo, New York 14263. *Received September 30, 1985*

Abstract: Two crystalline forms of *cyclo*-(D-Ala-Gly-L-Pro-L-Phe)$_2$, containing different peptide backbone conformations, have been subjected to X-ray crystallographic analysis. Both forms are in the orthorhombic space group $P2_12_12_1$. Form I, with dimensions a = 28.412 (2), b = 17.036 (2), and c = 8.959 (1) Å, contains one octapeptide molecule and two water molecules in the asymmetric unit. Its peptide backbone has only trans peptide bonds and approximate C_2 symmetry, with type I β turns at L-Pro-L-Phe. Except for the type I turns, this backbone is similar to that reported for *cyclo*-(D-Ala-Gly-L-Pro-D-Phe)$_2$, which has type II turns at L-Pro-D-Phe. Form II has dimensions a = 32.166 (2), b = 16.896 (2), and c = 8.156 (1) Å. Its asymmetric unit contains one octapeptide and six water molecules. The peptide backbone of form II also contains only trans peptide bonds and type I β turns at L-Pro-L-Phe but differs from that of form I in that the plane of one peptide bond joining Ala to Gly is rotated by about 180° relative to the local plane of α-carbons. Measurements of proton spin–lattice relaxation in the rotating frame, $T_{1\rho}$, were made on dimethyl sulfoxide solutions of *cyclo*-(D-Ala-Gly-L-Pro-L-Phe)$_2$, a peptide that is indicated to be conformationally mobile in solution by the ambiguity of the usual solution NMR observations. These were compared with similar measurements of *cyclo*-(D-Ala-Gly-L-Pro-D-Phe)$_2$, which previously reported studies indicated to have a more stable backbone conformation. Significantly shorter values of $T_{1\rho}$ for the former peptide represent contributions to relaxation of its protons by intramolecular motions in the 10^4–10^5-s^{-1} range.

Four diastereomeric cyclic octapeptides, *cyclo*-(D- or L-Ala-Gly-L-Pro-D- or L-Phe)$_2$, prepared in a search for new classes of conformationally stable cyclic peptide backbones, have been under study. Two of these, *cyclo*-(D-Ala-Gly-L-Pro-D-Phe)$_2$ and *cyclo*-(L-Ala-Gly-L-Pro-L-Phe)$_2$, were judged by NMR criteria to have conformationally stable all-trans backbones, and conformations were proposed for them on the basis of NMR measurements of dimethyl sulfoxide solutions.[1] A crystal structure of the D-Ala,D-Phe peptide, showing a backbone conformation similar to a likely solution conformation, has been reported.[2] The L-Ala-L-Phe isomer was proposed to have a backbone similar to that of β-amanitin[3] and an amanitin analogue.[4] In this paper we describe solution NMR studies and X-ray crystallographic analyses of the D-Ala,L-Phe diastereomer, *cyclo*-(D-Ala-Gly-L-Pro-L-Phe)$_2$.

The all-trans form of *cyclo*-(D-Ala-Gly-L-Pro-L-Phe)$_2$, which occurs to the extent of 90% in dimethyl sulfoxide solution, appears to possess a greater degree of conformational mobility than the D-Ala,D-Phe isomer. The indications are ambiguity of the usual solution NMR observations and the observation, reported here, of two different conformations in the crystalline state for the D-Ala,L-Phe peptide. It was therefore worthwhile to compare the two isomers with regard to proton spin–lattice relaxation in the rotating frame, $T_{1\rho}$, to determine if the increased mobility occurs on the time scale of motions particularly affecting $T_{1\rho}$, 10^{-4}–10^{-5} s in our studies. Faster $T_{1\rho}$ relaxation was indeed observed for the D-Ala,L-Phe peptide. These crystallographic and NMR results are presented below.

Experimental Procedures

The synthesis and characterization of *cyclo*-(D-Ala-Gly-L-Pro-L-Phe)$_2$ were described earlier.[1]

X-ray Analyses. Crystals of form I were grown by slow evaporation of a solution of the octapeptide in methanol–water. Form II was obtained by slow evaporation of a methanol–water solution containing sodium thiocyanate. Both forms crystallize in the orthorhombic space group $P2_12_12_1$ with unit cell dimensions a = 28.412 (2), b = 17.036 (2), and c = 8.959 (1) Å for form I and a = 32.166 (2), b = 16.896 (2), and c = 8.156 (1) Å for form II. Both forms contain 4 formula units, with a calculated density of 1.196 g/cm^3 for I and 1.278 g/cm^3 for II.

Intensity data to 2θ = 154° for both forms were measured with an Enraf-Nonius CAD-4 automatic diffractometer using Cu Kα (λ = 1.5418 Å) radiation. A crystal of size 0.3 × 0.2 × 0.4 mm, mounted in a capillary with mother liquor, was used to collect a total of 4989 independent reflections from form I. A crystal of form II, 0.3 × 0.4 × 0.5 mm, mounted on a glass fiber, was used to measure 5256 independent reflections. Intensity data were corrected for Lorentz-polarization effects, and an empirical absorption correction[5] was also applied.

Structures of both forms were solved by using the direct methods program MULTAN 80[6] and successive weighted Fourier maps. The asymmetric unit of form I contains one octapeptide and two water molecules for a total of 56 non-hydrogen atoms. That of form II contains one octapeptide and six water molecules, 60 non-hydrogen atoms.

The structure of form I was refined by the block-diagonal least-squares technique using 3145 reflections with $F_0 > 1.5\ \sigma F$. The atoms were treated isotropically in the initial stages and with anisotropic thermal parameters in the final stages of refinement. Hydrogen atom positions were calculated and included in the refinement in the final stages. The final R factor was 0.12 for 3145 reflections. The refinement and distance and angle calculations for form I were done by using local programs.

Form II was refined by the full-matrix least-squares technique using 3898 reflections with $I > 2\sigma I$. In the initial stages of refinement all the atoms were treated isotropically. Anisotropic thermal parameters were used in the final stages for all the atoms except OW6, which has very high isotropic temperature factor. Hydrogen atom positions were located from a difference map and were included in the calculation but not refined. The final R factor for form II was 0.058 for 3898 reflections. The final shift/error was 0.60, and the goodness-of-fit parameter was

† Illinois Institute of Technology. Present address: Smith Kline & French Laboratories, Philadelphia, PA 19101.
‡ Roswell Park Memorial Institute.
§ Deceased 1984.
‖ Illinois Institute of Technology.

(1) Kopple, K. D.; Parameswaran, K. N.; Yonan, J. P. *J. Am. Chem. Soc.* **1984**, *106*, 7212–7217.
(2) Kopple, K. D.; Kartha, G.; Bhandary, K. K.; Romanowska, K. *J. Am. Chem. Soc.* **1985**, *107*, 4893–4897.
(3) Kostansek, E. C.; Lipscomb, W. N.; Yocum, R. R.; Thiessen, W. E. *Biochemistry* **1978**, *17*, 3790–3975.
(4) Shoham, G.; Rees, D. C.; Lipscomb, W. N.; Zanotti, G.; Wieland, Th. *J. Am. Chem. Soc.* **1984**, *106*, 4606–4615.
(5) North, A. C. T.; Phillips, D. C.; Matthews, F. C. *Acta Crystallogr., Sect. A: Cryst. Phys., Diffr., Theor. Gen. Crystallogr.* **1968**, *A24*, 351–359.
(6) Main, P.; Hull, S. E.; Lessinger, L.; Germain, G.; DeClarq, J.-P.; Woolfson, M. M. MULTAN 80, A System of Computer Programs for the Automatic Solution of Crystal Structures from X-ray Diffraction Data; Universities of York and Louvain: York, England, and Louvain, Belgium, 1980.

0002-7863/86/1508-4637$01.50/0

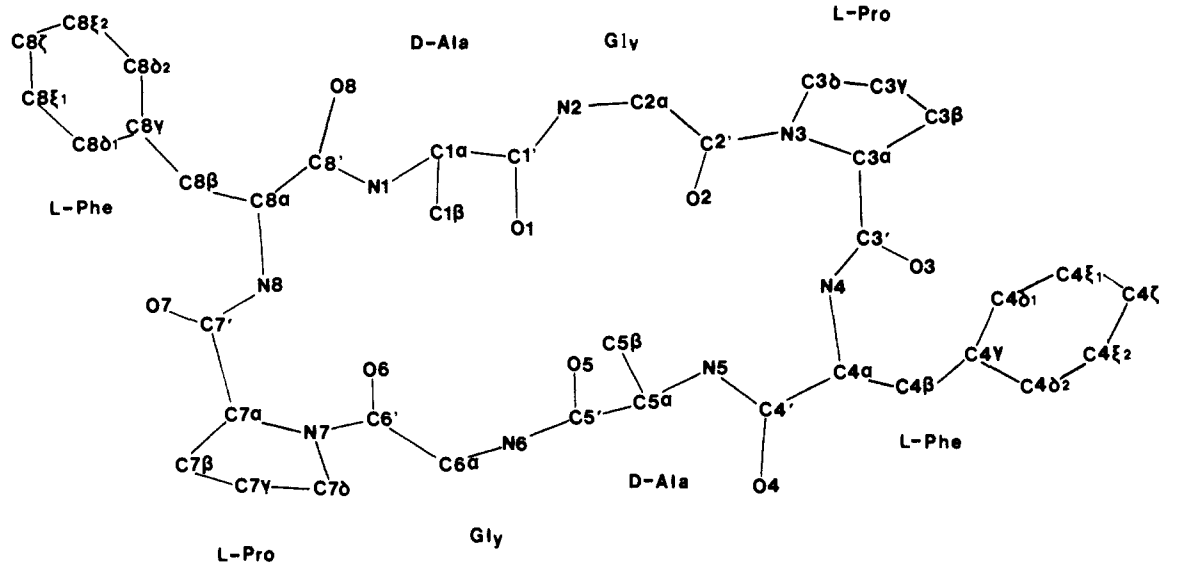

Figure 1. Numbering scheme used for the cyclic octapeptides.

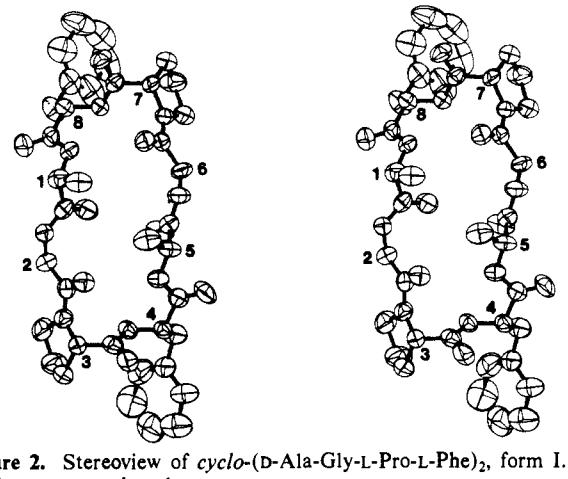

Figure 2. Stereoview of *cyclo*-(D-Ala-Gly-L-Pro-L-Phe)$_2$, form I. α-Carbons are numbered.

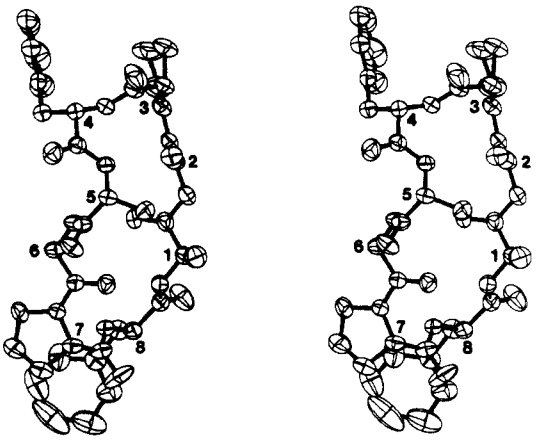

Figure 3. Stereoview of *cyclo*-(D-Ala-Gly-L-Pro-L-Phe)$_2$, form II. α-Carbons are numbered.

1.42. The calculations for form II were carried by using the Structural Data Package. The final atomic coordinates and structure factor tables for both the forms are available as supplementary material.

NMR Measurements. ^{1}H NMR data were obtained by using a Nicolet NT-300 spectrometer, operating at 300 MHz for protons and 75 MHz for carbon. Peptide concentrations were 10 mM or less for proton spectra and 10–25 mM for carbon spectra. Proton $T_{1\rho}$ measurements were made at 20° on 7 mM degassed sealed samples in 5-mm tubes. Excitation and spin-locking power were obtained from the low-power transmitter of the spectrometer augmented by an ENI 10-W linear amplifier. The usual 90_x–t(SL$_y$) acquisition sequence was used. A pair of crossed diodes at the amplifier output reduced noise during acquisition. To ensure that accurate $T_{1\rho}$ values were obtained, the protons examined had resonances free of overlaps, and separate experiments, with the locking field, H_1, at the Larmor frequency of each proton, were made for each proton. Relaxation measurements were made at five or six different field strengths between $\gamma(H_1)$ = 2600 and 8600 Hz, using at least 10 spin-locking times between 6 ms and 2 s. Values of $T_{1\rho}$ were obtained by fitting resonance intensities to the expression $I = I_0 \exp(-t_{SL}/T_{1\rho}) + I_r$, where I_r represents a residual signal present at long spin-locking times ($>10T_{1\rho}$), usually $<0.03I_0$. Proton and carbon-13 T_1 values were obtained by inversion–recovery, again using 10 or more recovery times and fitting the resonance intensities to the expression $I = I_0(1 + W) \times \exp(-t/T_1)$, where W may be less than 1, to take into account incomplete inversion due to H_1 inhomogeneity.

Results

Crystal Structures. The numbering scheme used is shown in Figure 1. Final positional and thermal parameters are included in the supplementary material. The bond lengths (Table IA) and angles (Table IB) agree well within experimental error in the two structures and compare well with values in the literature,[7] except for the values for the three end atoms of the phenyl group that show relatively high thermal motion. Torsional angles for the two

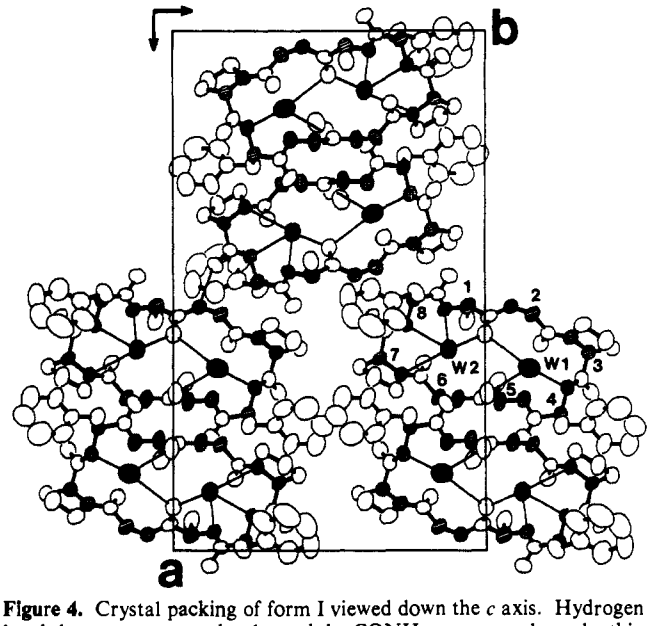

Figure 4. Crystal packing of form I viewed down the c axis. Hydrogen bonds between water molecules and the CONH groups are shown by thin lines. The α-carbons (banded) of one molecule are numbered. The nitrogen atoms are crosshatched, and the water molecules are fully shaded.

Table I. Bond Lengths[a] (Å) and Bond Angles[b] (deg) for *cyclo*-(D-Ala-Gly-L-Pro-L-Phe)$_2$, Form I (Form II)

	D-Ala (i = 1)	Gly (i = 2)	L-Pro (i = 3)	L-Phe (i = 4)	D-Ala (i = 5)	Gly (i = 6)	L-Pro (i = 7)	L-Phe (i = 8)
				(A) Bond Lengths				
Ni–C$i\alpha$	1.490	1.431	1.435	1.458	1.422	1.471	1.505	1.445
	(1.459)	(1.457)	(1.469)	(1.444)	(1.457)	(1.451)	(1.478)	(1.460)
C$i\alpha$–C′i	1.559	1.555	1.483	1.529	1.550	1.501	1.533	1.525
	(1.512)	(1.513)	(1.529)	(1.512)	(1.517)	(1.532)	(1.484)	(1.528)
C′i–Oi	1.240	1.240	1.212	1.185	1.183	1.188	1.212	1.239
	(1.238)	(1.220)	(1.220)	(1.231)	(1.229)	(1.221)	(1.230)	(1.225)
C′i–Ni+1	1.289	1.357	1.357	1.348	1.314	1.340	1.343	1.327
	(1.323)	(1.357)	(1.348)	(1.340)	(1.338)	(1.350)	(1.327)	(1.338)
C$i\alpha$–C$i\beta$	1.496		1.501	1.541	1.510		1.480	1.487
	(1.495)		(1.518)	(1.550)	(1.533)		(1.530)	(1.546)
C$i\beta$–C$i\gamma$			1.506				1.507	
			(1.458)				(1.480)	
C$i\gamma$–C$i\delta$			1.431				1.562	
			(1.554)				(1.459)	
C$i\delta$–Ni			1.474				1.475	
			(1.461)				(1.460)	
C$i\beta$–C$i\gamma$				1.485				1.503
				(1.514)				(1.486)
C$i\gamma$–C$i\delta_1$				1.399				1.337
				(1.387)				(1.373)
C$i\delta_1$–C$i\epsilon_1$				1.447				1.409
				(1.404)				(1.400)
C$i\epsilon_1$–Ci				1.374				1.227
				(1.402)				(1.346)
C$i\zeta$–C$i\epsilon_2$				1.364				1.376
				(1.369)				(1.384)
C$i\epsilon_2$–C$i\delta_2$				1.374				1.555
				(1.402)				(1.346)
C$i\delta_2$–C$i\gamma$				1.364				1.376
				(1.369)				(1.384)
				(B) Bond Angles				
C′i-1–Ni–C$i\alpha$	121	124	117	123	121	121	122	123
	(122.5)	(122.5)	(119.3)	(120.7)	(121.1)	(119.8)	(120.6)	(123.5)
C$i\alpha$–Ni–C$i\delta$			114				111	
			(112.7)				(112.5)	
C′i-1–Ni–Cδ			128				127	
			(127.1)				(126.4)	
C′i–C$i\alpha$–Ni	109	115	115	113	107	113	114	111
	(110.2)	(111.8)	(115.0)	(113.1)	(112.6)	(110.8)	(115.3)	(111.7)
Ni–C$i\alpha$–C$i\beta$	110		102	111	109		104	116
	(109.7)		(103.2)	(109.9)	(109.1)		(102.3)	(111.8)
C$i\alpha$–C′i–Oi	120	122	121	121	124	122	118	119
	(122.5)	(123.0)	(119.5)	(120.4)	(120.4)	(123.1)	(117.9)	(120.4)
C$i\beta$–C$i\alpha$–C′i	110		111	109	114		113	110
	(111.2)		(112.5)	(108.2)	(110.1)		(111.7)	(110.7)
Ni+1–C′i–C$i\alpha$	114	115	117	117	112	114	117	118
	(115.1)	(115.0)	(116.6)	(117.9)	(118.1)	(114.6)	(120.1)	(117.5)
Ni+1–C′i–Oi	125	123	122	122	124	124	125	123
	(122.4)	(122.0)	(124.0)	(121.7)	(121.5)	(122.3)	(122.0)	(122.1)
C$i\alpha$–C$i\beta$–C$i\gamma$			106				106	
			(104.3)				(105.7)	
C$i\beta$–C$i\gamma$–C$i\delta$			106				103	
			(105.2)				(107.4)	
C$i\gamma$–C$i\delta$–Ni			102				103	
			(100.7)				(103.7)	
C$i\alpha$–C$i\beta$–C$i\gamma$				114				109
				(113.0)				(110.2)
C$i\beta$–C$i\gamma$–C$i\delta_1$				122				127
				(121.5)				(120.7)
C$i\beta$–C$i\gamma$–C$i\delta_2$				122				121
				(120.2)				(121.2)
C$i\delta_2$–C$i\gamma$–C$i\delta_1$				116				111
				(118.3)				(118.2)
C$i\gamma$–C$i\delta_1$–C$i\epsilon_1$				119				132
				(120.2)				(121.9)
C$i\delta_1$–C$i\epsilon_1$–C$i\zeta$				117				111
				(120.6)				(118.0)
C$i\epsilon_1$–C$i\zeta$–Ci_2				124				132
				(119.2)				(118.6)
C$i\zeta$–C$i\epsilon_2$–Clδ_2				120				115
				(121.9)				(123.8)
Clϵ_2–Clδ_2–Clγ				124				118
				(119.9)				(119.7)

[a] Average esd for bond length is 0.009 (0.006) Å. [b] Average esd for bond angles is 1 (0.5)°.

Table II. Conformational Angles (deg) for Crystalline *cyclo*-(D-Ala-Gly-L-Pro-L-Phe)$_2$, Form I (Form II)

angle[a]	D-Ala (i = 1)	Gly (i = 2)	L-Pro (i = 3)	L-Phe (i = 4)	D-Ala (i = 5)	Gly (i = 6)	L-Pro (i =7)	L-Phe (i =8)
ϕ	82	95	−70	−98	79	124	−68	−116
	(97)	(88)	(−76)	(−90)	(69)	(−71)	(−69)	(−111)
ψ	−155	169	−24	14	179	175	−15	14
	(−161)	(172)	(−14)	(1)	(31)	(173)	(−13)	(13)
ω	−178	−170	180	180	178	−172	−177	−175
	(−175)	(−168)	(180)	(−177)	(172)	(−172)	(178)	(−177)
χ^0			−1				−7	
			(−8)				(−3)	
χ^1			20	−65			27	−49
			(28)	(−53)			(19)	(−62)
χ^2			−34	−73			−36	−70
			(−38)	(−70)			(−29)	(−82)
χ^3			32				31	
			(32)				(27)	
χ^4			−20				−15	
			(−14)				(−15)	

[a] Main chain: ϕ, C′i-1–Ni–C$i\alpha$–C′i; ψ, Ni–C$i\alpha$–C′i–Ni + 1; ω, C$i\alpha$–C′i–Ni + 1–Ci + 1α. Pro: χ^0, C$i\delta$–Ni–C$i\alpha$–C$i\beta$; χ^1, Ni–C$i\alpha$–C$i\beta$–C$i\gamma$; χ^2, C$i\alpha$–C$i\beta$–C$i\gamma$–C$i\delta$; χ^3, C$i\beta$–C$i\gamma$–C$i\delta$–Ni; χ^4, C$i\gamma$–C$i\delta$–Ni–C$i\alpha$. Phe: χ^1, Ni–C$i\alpha$–C$i\beta$–C$i\gamma$; χ^2, C$i\alpha$–C$i\beta$–C$i\gamma$–C$i\delta_1$.

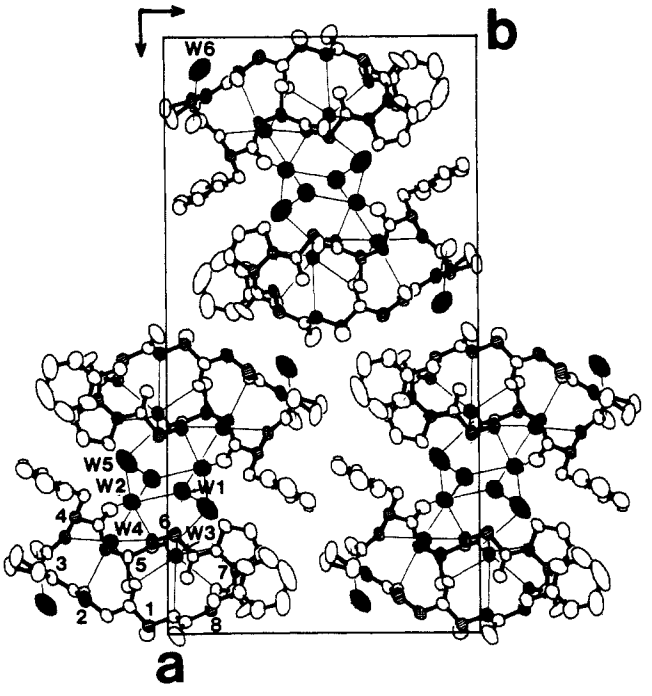

Figure 5. Crystal packing of form II viewed down the c axis. Conventions are as in Figure 4.

structures are given in Table II. Figures 2 and 3 show the peptide conformations of both forms, and Figures 4 and 5 show the crystal packings. Inter- and intramolecular hydrogen-bond distances below 3.2 Å are listed in Table III.

In both forms all the peptide links are trans. Values of the C′–N dihedral angle ω deviate from 180° by no more than 10° in form I and no more than 12° in form II. Both forms contain two type I L-Pro-L-Phe β turns (mean values of ϕ, ψ: ca. −71°, −16°; −104°, 11°) linked by D-Ala-Gly sequences. The four Phe-Pro β turns have closely similar conformational angles for side chains and backbone. The Pro rings all have Cγ-exo puckering, and χ^1 for all Phe residues is near −60°.

Although differences as large as 29° (in ϕ_{Gly}) occur between equivalent torsion angles, form I of *cyclo*-(D-Ala-Gly-L-Pro-L-Phe)$_2$ has an overall approximate C_2 symmetry, and its octapeptide ring is flatter than that of *cyclo*-(D-Ala-Gly-L-Pro-D-Phe)$_2$. If its backbone is described as consisting of two approximate planes formed by the α-carbons of Ala-Gly-Pro-Phe-Ala sequences joined at the Ala α-carbons, the dihedral angle between these planes is 148°. This is in contrast to 94° for the corresponding angle in the D-Ala,D-Phe isomer, which also differs, of course, in possessing type II L-Pro-D-Phe β turns.[2]

Although there are no good intramolecular N–H···O contacts in form I, its backbone conformation may be stabilized by two water molecules, each of which forms hydrogen bonds to the NH proton of a Phe and the carbonyl oxygen of the succeeding Ala. These water molecules occupy the center of the peptide molecule and are not involved in hydrogen bonding between peptide molecules. The peptide molecules form columns parallel to the c axis. (See Figure 4.) There is one good interpeptide hydrogen bond [N···O distance 2.810 (7) Å] between a Gly NH and a Pro carbonyl of a symmetry-related molecule.

The principal difference between the backbones of forms I and II occurs at one of the Ala–Gly links of II. In half of the form II peptide, ψ_{Ala_n} is −161°, which is near the values −155 and 179° found in form I, and $\phi_{Gly_{n+1}}$ is 88°, near the 95 and 124° of form I. However, in the other half, the plane of this peptide link is rotated so that ψ_{Ala} = 31° and ϕ_{Gly} = −71°. Otherwise, the shapes of the backbones in the two forms are very similar. The dihedral

Table III. Hydrogen-Bond Distances (Å) in *cyclo*-(D-Ala-Gly-L-Pro-L-Phe)$_2$ below 3.2 Å

atom 1	atom 2	symmetry[a]	dist (esd)
		Form I	
O1	OW2	I (0, 0, 0)	2.757 (9)
N2	O7	IV (1, 0, 0)	2.810 (7)
O2	N5	I (0, 0, 0)	3.177 (9)
N4	OW1	I (0, 0, 0)	3.02 (1)
O5	OW1	I (0, 0, 0)	3.01 (1)
O6	N8	I (0, 0, 0)	3.155 (9)
N8	OW2	I (0, 0, 0)	2.931 (7)
		Form II	
N1	O6	I (0, 0, 0)	3.088 (6)
O1	OW3	I (0, 0, 0)	2.765 (5)
O1	OW4	I (0, 0, 0)	2.725 (5)
N2	O7	IV (2, −1, 1)	2.692 (6)
O3	OW6	IV (1, −1, 0)	3.15 (1)
N4	OW4	I (0, 0, 0)	3.065 (6)
O4	OW2	I (0, 0, −1)	2.844 (6)
O4	OW1	II (1, 0, −1)	3.140 (7)
O5	OW3	I (0, 0, −1)	2.701 (5)
O5	OW5	II (1, 0, −1)	2.737 (7)
N6	OW4	I (0, 0, 0)	3.064 (5)
O6	N8	I (0, 0, 0)	3.106 (5)
N8	OW3	I (0, 0, 0)	2.853 (5)
O8	OW6	I (1, 0, 1)	2.77 (1)
OW1	OW2	I (0, 0, 0)	2.772 (6)
OW1	OW5	II (1, 0, 0)	2.750 (9)
OW2	OW4	I (0, 0, 0)	2.813 (6)
OW2	OW5	I (0, 0, 0)	2.938 (7)

[a] Symmetry: I, x, y, z; II, $^1/_2 - x$, $-y$, $^1/_2 + z$; III, $^1/_2 + x$, $^1/_2 - y$, $-z$; IV, $-x$, $^1/_2 + y$, $^1/_2 - z$.

(7) Benedetti, E. In *Peptides, Proceedings of the 5th American Peptide Symposium*; Goodman, M., Meienhofer, J., Eds.; Wiley: New York, 1977; pp 257–253.

Table IV. NMR Data for *cyclo*-(D-Ala-Gly-L-Pro-L-Phe)$_2$ in Me_2SO, 23 °C

NH Protons		α-Protons	
	Ala	δ(Ala)	4.19
δ	7.42	δ(Gly) (^2J)	3.99 (16.5)
$d\delta/dT^a$	−0.0015		3.78
$k_{nitroxyl}{}^b$	80	δ(Pro)	4.07
J_{HNCH}	7.6	δ(Phe)	4.26
	Gly	β-Protons	
δ	7.51	δ(Phe) ($J_{\alpha\beta}$)	3.23 (3.8)
$d\delta/dT^a$	−0.0015		2.89 (11.6)
$k_{nitroxyl}{}^b$	150	δ(Pro)	1.95, 1.41
$J_{HNCH}{}^c$	5.1, 6.1	Carbons	
	Phe	δ(Pro β)	28.76
δ	8.07	δ(Pro γ)	24.31
$d\delta/dT^a$	−0.0046		
$k_{nitroxyl}{}^b$	170		
J_{HNCH}	7.7		

[a] Chemical shift temperature coefficient (ppm/deg). Negative coefficients correspond to shift upfield with increasing temperature. [b] Second-order rate constant (M^{-1} s^{-1}) for T_1 relaxation by 2,2,6,6-tetramethylpiperidinyl-1-oxy (TEMPO). [c] Coupling to higher field α-proton given first.

angle between the two average Ala-Gly-Pro-Phe-Ala α-carbon planes in form II is 140°.

In form II there are again no good intramolecular N–H···O hydrogen bonds, but as in form I there is one interpeptide hydrogen bond [N···O distance 2.692 (6) Å] between a Gly NH and a symmetry-related Pro carbonyl. There are six water molecules per octapeptide. One of them bridges between Ala carbonyl O1 and Phe N8 as in form I. The rotation of the Ala^5–Gly^6 peptide bond plane that takes the conformation of form I into that of form II has the effect of increasing the exposure of the Ala carbonyl oxygen, O5, allowing it to form two good hydrogen bonds to external water molecules. However, it is probably not correct to point to this single interaction as the driving force for the conformation change, since Ala carbonyl O1, which is in the same peptide environment as it is in form I, also forms an additional good hydrogen bond to a nonbridging water molecule.

The peptide molecules of form II form columns parallel to the *c* axis like those of form I, and water molecules form parallel columns between the peptide columns. The waters of these columns are extensively involved in hydrogen bonds among themselves and with peptide carbonyls. (See Figure 5.) Parallel peptide and water columns are a feature of other peptide crystals.[8,9]

NMR Studies of Solution Conformation. The dominant form of *cyclo*-(D-Ala-Gly-L-Pro-L-Phe)$_2$ in dimethyl sulfoxide solution has C_2 symmetry in the NMR time average. On the evidence of the 4.5 ppm chemical shift separation of the proline β- and γ-carbon resonances, it has *trans*-Gly–Pro peptide bonds.[10] Approximately 10% of the peptide is present in second form with one *cis*-Gly–Pro bond. Conformationally significant NMR observations of the major form are reported in Table IV. No nuclear Overhauser effects greater than 2% could be observed among its backbone protons.

The spectrum of the D-Ala,L-Phe analogue lacks features that suggest a single narrowly defined backbone conformation, in contrast to the spectra of the D-Ala,D-Phe and L-Ala,L-Phe diastereomers described earlier. For example, the chemical shift nonequivalence of the glycine α-protons is only 0.21 ppm, compared to 0.46 ppm in the D-Ala,D-Phe peptide and 0.64 ppm in the L-Ala,L-Phe analogue, which suggests more comprehensive averaging of the position of the glycine methylene relative to the magnetically anisotropic CONH groups flanking it. Also, there are no extreme values of H–N–C–H and H–C–H coupling constants as are found in the L,L case (in the L-Ala,L-Phe peptide, $^3J_{HNCH}$ = <2 and 7.8 Hz for Gly and 8.8 for Ala, and $^2J_{HCH}$ = 17.8 for Gly), and there is no wide range of NH chemical shifts as in the D,D compound (1.93 ppm). Therefore, although a set of constraints could be derived from the NMR data, a model derived from them was not considered likely to represent a single conformation dominant in solution. Table V compares observed values with those expected for two conformations of the tetrapeptide sequence -L-Phe-D-Ala-Gly-L-Pro- found in the crystals: A, the conformation of the approximately C_2 symmetric form I; B, the different conformation found in half of form II. Examination of Table V will show that the NMR observations do not point to one or the other crystal conformation, to a particular averaged combination of them, or to some other conformational average. In the absence of any clear indication that defines a single conformation, it is most reasonable to assume that in solution the all-trans form of *cyclo*-(D-Ala-Gly-L-Pro-L-Phe)$_2$ is conformationally mobile.

Table V. NMR Observations and the Values Expected for the Crystal Conformations of the -L-Phe-D-Ala-Gly-L-Pro- Sequences

	conformation[a]		
	A	B	obsd
L-Phe			
ϕ	−(90–120)	−110	
J^b	7.5–9	8.5	7.7
D-Ala			
ϕ	80–100	70	
J^b	6.5–8.5	5	7.6
Gly			
ϕ	90–120	−70	
J (*pro-R*)^b	3–5	5	(5.1)
J (*pro-S*)^b	7.5–9.5	6	(6.1)
ψ	170–175	170	
J^c	17–18	17.5	16.5
L-Pro			
ψ	10–25	15	
$\Delta\delta_{\beta\gamma}{}^d$	3.5	3.5	4.5

[a] Crystal dihedral angles (deg) rounded to nearest 5°. Estimated coupling constants (Hz) rounded to nearest 0.5 Hz and chemical shift difference to 0.5 ppm. [b] $^3J_{HNCH}$ estimated from range of crystal dihedral angles and range of coupling constants predicted therefrom by the correlations of: Ramachandran, G. N.; Chandrasekaran, R.; Kopple, K. D. *Biopolymers* **1971**, *10*, 2113–2131. DeMarco, A.; Llinas, M.; Wütrich, K. *Biopolymers* **1978**, *17*, 637–650. [c] $^2J_{HCH}$ estimated from range of crystal angles using correlation of: Barfield, M.; Hruby, V. J.; Meraldi, J. P. *J. Am. Chem. Soc.* **1976**, *98*, 1308–1314. [d] Estimated from crystal angles according to ref 10.

Rotating-Frame Relaxation Studies. From this ambiguity of the NMR observations, the backbone of the all-trans form of *cyclo*-(D-Ala-Gly-L-Pro-L-Phe)$_2$ appears to be conformationally mobile. In distinction, the earlier reported observations of the all-trans form of the D-Ala,D-Phe diasteroisomer suggest that its backbone conformation in solution is more narrowly defined. However, for both peptides any conformational interconversions, excluding cis–trans isomerism at Gly–Pro, are faster than about 10^2 s^{-1}, and only one set of narrow (averaged) resonances is observed, which is usual for oligopeptides.

With the expectation that a difference in internal motion between the two peptides might be apparent on a shorter time scale, we measured spin–lattice relaxation in the rotating frame ($T_{1\rho}$) for backbone NH protons in both peptides. Exchange between conformations that result in fluctuations in chemical shift or spin–spin coupling can result in contributions to the $T_{1\rho}$ relaxation rate.[11,12] These will be maximal when the exchange occurs at a rate near the frequency corresponding to the spin-locking field $\gamma(H_1)$ used in the $T_{1\rho}$ experiment. This is commonly of the order of 10^4–10^5 s^{-1}, well into the fast-exchange region on the chemical shift time scale. Bleich and Glasel[13,14] have previously discussed

(8) Chiang, C. C.; Karle, I. L.; Wieland, Th. *Int. J. Pept. Protein Res.* **1982**, *20*, 414–420.
(9) Hossain, M. B.; van der Helm, D. *J. Am. Chem. Soc.* **1978**, *100*, 5191–5198.
(10) Siemion, I. Z.; Wieland, T.; Pook, K.-H. *Angew. Chem., Int. Ed. Engl.* **1975**, *14*, 702–703.
(11) Deverell, C.; Morgan, R. E.; Strange, J. H. *Mol. Phys.* **1970**, *18*, 553–559.
(12) Strange, J. H.; Morgan, R. E. *J. Phys. C* **1970**, *3*, 1999–2011.
(13) Bleich, H. E.; Glasel, J. A. *Biopolymers* **1978**, *17*, 2445–2457.

Table VI. Proton Relaxation Rates (s^{-1}) for *cyclo*-(?-Ala-Gly-L-Pro-?-Phe)$_2$ in Me_2SO at 20 °C

	D-Ala,L-Phe			D-Ala,D-Phe		
	$R_{1\rho}$[a]	R_1	$R_{1\rho}$(exch)[b]	$R_{1\rho}$[a]	R_1	$R_{1\rho}$(exch)[b]
Ala NH	10.6	2.9	5.9	8.1	3.1	2.9
Gly NH	11.1	3.0	6.2	8.3	2.7	3.8
Phe NH	12.5	3.1	7.5	8.8	3.4	3.2

[a] Observed relaxation rate at $\gamma(H_1)$ = 8333 Hz, about 2 W into the probe and interface used. The standard error for $T_{1\rho}$ was consistently about ±0.003 s. [b] Calculated as outlined in the text. Error propagated from the 0.003-s error in $T_{1\rho}$ (obsd) amounts to ±7% in $R_{1\rho}$ (exch). An additional error of about ±0.4 s^{-1} is estimated principally from the uncertainty in the estimate of τ_c from ^{13}C T_1 values.

the use of $T_{1\rho}$ for studies of peptide conformational mobility. Because of the sensitivity of their chemical shifts to hydrogen-bonding effects and thus to conformational exchange, the peptide NH proton resonances are most appropriate for $T_{1\rho}$ examination. In contrast to $T_{1\rho}$, the more commonly measured T_1 is sensitive to fluctuations near the Larmor frequency in the static field, which is in the 10^9–s^{-1} range. T_1 is thus determined by the rotational correlation time, which is ca. 10^{-10} for peptides of this size, and it does not reflect any slower motions that may be present.

Table VI reports the relaxation rates $1/T_1$ and $1/T_{1\rho}$ of the NH protons at a spin-locking field for the $T_{1\rho}$ experiments of 5.2 × 10^4 rad s^{-1}. It is seen that the laboratory frame spin–lattice relaxation rates are about the same for the two peptides and that the rotating-frame relaxation rates are higher for both peptides, but by a significantly larger amount for the D-Ala,L-Phe peptide.

There are three likely contributions to the larger rotating-frame relaxation rates. First, if the rotational correlation time of these molecules is sufficiently long ($\gamma(H_0) > 1/\tau_c > \gamma(H_1)$), the dipole–dipole coupling mechanism will yield $1/T_{1\rho}$ larger than $1/T_1$. This turns out to be the case in the present examples. Second, there is scalar relaxation. Modulation of the NH coupling by ^{14}N relaxation (scalar relaxation of the second kind) can contribute to $1/T_{1\rho}$. Scalar relaxation of the first kind, modulation of coupling to the observed protons by exchange, can be shown to be less important in the present examples. The third source of rotating-frame relaxation, and the one of interest here, is modulation of the Larmor frequency by exchange of nuclei among sites of different chemical shift. In the present case this will be a result of conformational exchange, proton exchange being very slow in Me_2SO. The observed $T_{1\rho}$ can thus be expressed as

$$\frac{1}{T_{1\rho}(\text{obsd})} = \frac{1}{T_{1\rho}(\text{dd, H})} + \frac{1}{T_{1\rho}(\text{dd, N})} + \frac{1}{T_{1\rho}(\text{Sr})} + \frac{1}{T_{1\rho}(\text{exch})}$$

The first three relaxation rates on the right can be estimated for a given spin-locking field as follows. The contributions of the directly bound nitrogen to T_1 and $T_{1\rho}$ relaxations can be calculated, given a knowledge of the rotational correlation time τ_c for the peptide backbone. This is taken as the isotropic value calculated from the proton-decoupled T_1 relaxation rate of the α-carbons. The laboratory frame (T_1) dipolar relaxation rate due to protons can be obtained by subtracting the T_1 rate due to nitrogen, and the ratio of this to the rotating frame dipolar relaxation rate can be calculated, given the knowledge of τ_c. The relaxation rate of the nitrogen by the dominant quadrupolar mechanism can be calculated from knowledge of τ_c and estimate of the quadrupolar coupling constant of amide nitrogen, taken here as the reported value for formamide.[15] From the nitrogen relaxation rate and the N–H coupling constant the scalar relaxation term can be calculated. Details of these calculations will be given in a later paper, but representative values of the rates ($R_i = 1/T_i$) are given below for the spin-locking field of 8333 Hz used here.

$$\tau_c(\text{backbone}) = 4 \times 10^{-10}\ \text{s};\ \tau_N = 1.3 \times 10^{-3}\ \text{s}$$

$$R_1(\text{dd, N}) = 0.75\ s^{-1};\ R_{1\rho}(\text{dd, N}) = 0.95\ s^{-1}$$

$$R_1(\text{dd, H}) = 3.5\text{–}4.8\ s^{-1};\ R_{1\rho}(\text{dd, H})/R_1(\text{dd, H}) = 1.75$$

$$R_{1\rho}(\text{sr II}) = 0.0007\ s^{-1}$$

Table VI gives T_1 and $T_{1\rho}$ rates for the NH protons and the chemical-exchange component of the $T_{1\rho}$ rates. It should be noted that proton transfer is too slow in these Me_2SO solutions to add to this exchange-induced relaxation. The T_1 relaxation rates, dependent on the rotational correlation time and interproton distances, and thus on the general size and shape of the peptides, are similar for the two diastereomers. There are exchange contributions to the $T_{1\rho}$ rate for both peptides, so that both must have internal mobility effective on the $T_{1\rho}$ time scale, but these exchange contributions are distinctly different, those in the D-Ala,L-Phe peptide being about twice as large as those in the D,D isomer.

In the absence of a specific model for the conformational exchange, including NH proton chemical shifts and populations of the conformations involved, these residual relaxation rates cannot be interpreted in detail. To generalize, however, the larger exchange contributions for the D,L peptide may arise from greater chemical shift differences between conformational states, which could reasonably be associated with larger variations in conformation. A second possibility is that internal motion in the D,L peptide could have larger low-frequency components. This, too, might correlate with larger excursions of atomic groups.

Measurements made at varying spin-locking fields show that for the D,D peptide the exchange contribution is not H_1 dependent, indicating a characteristic time for conformation exchange on the high-frequency side of our highest $\gamma(H_1)$, 5.2 × 10^4 s^{-1}. A slight field dependence for the D,L peptide suggests that it may have some lower frequency components.

The rotating-frame relaxation measurements are consistent with the indications from chemical shift, solvent exposure, and coupling constant data that the D,L peptide is the more flexible isomer. $T_{1\rho}$ measurements may thus allow investigation of internal mobility as an additional dimension in peptide conformation. Further work along these lines is in progress.

Acknowledgment. This work was supported by grants from the National Institutes of Health (GM 22490 to G.K. and K.K.B and 26071 to K.D.K.).

Supplementary Material Available: Tables of observed and calculated structure factors for *cyclo*-(D-Ala-Gly-Pro-Phe)$_2$·2H_2O, form I, and for *cyclo*-(D-Ala-Gly-Pro-Phe)$_2$·6H_2O, form II (38 pages). Ordering information is given on any current masthead page.

(14) Bleich, H. E.; Day, A. R.; Freer, R. J.; Glasel, J. A. *Biochem. Biophys. Res. Commun.* **1979**, *87*, 1146–1153.

(15) Guibe, L.; Lucken, A. C. *C. R. Hebd. Seances Acad. Sci., Ser. B* **1966**, *263*, 815–818.